Catalysis Today 238 (2014) 2–9

Contents lists available at ScienceDirect

Catalysis Today

journal homepage: www.elsevier.com/locate/cattod

Oxygen activation on oxide surfaces: A perspective at the atomic level

Hans-Joachim Freund*

Fritz-Haber-Institut der Max-Planck Gesellschaft, Faradayweg 4-6, 14195 Berlin, Germany

ARTICLE INFO

Article history:
Received 5 March 2014
Received in revised form 19 May 2014
Accepted 20 May 2014
Available online 2 July 2014

Keywords:
Oxygen activation
Oxide surfaces
Adsorption

ABSTRACT

Thin oxide films have been used as model supports to unravel the influence of the oxide–metal and oxide–gas interface. We discuss the influence of defects in the oxide lattice and the oxide surface on properties of adsorbed species, in particular the formation of oxide particles from a deposited transition metal onto ceria and of adsorbed oxygen from the gas phase. Here we correlate the structure of the particles, as revealed by a combination of STM and spectroscopic as well as theoretical calculations, with their reactive properties. The nature of the involved defects is characterized by adsorption of Au as a way to correlate the influence of various defects of different structure on the Au charge state. In a second case study, we demonstrate the influence of dopants within the supporting oxide on the adsorption of oxygen on a defect free surface. This is shown to be potentially relevant for the activation of methane in oxidative methane coupling reactions, as recently demonstrated.

1. Introduction

Adsorption on defect-free oxides is generally weak given the high degree of bond saturation at their surface and the large gap, in particular, that governs their electronic structure [14,15,24,26,31,38,44,45,52–54,58]. Metal atoms deposited onto pristine oxides have essentially two means to interact with the surface [58]. The first one, being accessible to all atoms, arises from van der Waals or dispersive forces, i.e., the adatom gets polarized in the Madelung field of the oxide and experiences dipolar coupling to the surface. Depending on the atom polarizability, the resulting adsorption energies are of the order of 0.5 eV or below for a single atom. The second interaction channel that is relevant for open-shell d- and f-elements is direct hybridization between orbitals of the adspecies and the oxide surface. Especially the overlap between the d-states of transition metal atoms and the 2p orbitals of the surface oxygen plays an important role and enables an increase in the metal-oxide bond strength to more than 1.0 eV [27,28,57]. Naturally, this channel is dominant for metals with partly filled d-shells (Cr, Mn, Fe, V) and loses influence for semi-noble and noble metals, e.g., Pt, Cu, Ag, and Au. Oxide materials are never perfect and therefore surface defects need to be considered as potential binding sites for any adsorbate (ref. J. Haber in [10]). In particular, with respect to oxidation of hydrocarbons, the interaction of oxygen from the gas phase with surface defects has been considered essential for oxygen binding to the surface, forming the so called “electro-phyllic” oxygen, while the lattice oxygen was considered to be “nucleo-phyllic”. According to a proposal by Callahan and Grasselli [5], the concentration of “Nucleo-phyllic” lattice oxygen in direct contact with the active center, controls the selectivity of the catalytic reaction with respect to total oxidation. They called this scenario “site isolation principle”. The active centers may be associated with oxide defects.

Oxide defects often give rise to considerable variations in the electrostatic potential, which originate from unbalanced charges and cannot be screened due to the low density of free carries in the insulating material. In covalently bound oxides, dangling bond states may emerge at the defect site, reflecting the rigid lattice structure of the system that does not support bond reorganization. Whereas dangling bond states are highly susceptible to form covalent bonds to metal adatoms, electrostatic forces and charge transfer processes become relevant in the presence of charged defects in ionic oxides. Oxygen vacancies in MgO, for example, are able to exchange electrons with metallic adsorbates, which enable strong Coulomb attraction between both partners. Defect-mediated interaction schemes exceed the binding potential of the regular surface by up to a factor of three, underlining the significance of such lattice irregularities for the nucleation and growth of metals on oxide materials and adsorption in general. A particularly interesting approach to modify the adsorption strength without generating surface defects is the insertion of charge sources directly into the oxide lattice (Fig. 1).

In such a scenario, doping with aliovalent impurity ions may be exploited to introduce charges into the interior of thick films and even bulk oxides. Also in this case, charge transfer into the

* Tel.: +49 30 8413 4100; fax: +49 30 8413 4101.
E-mail address: freund@fhi-berlin.mpg.de

http://dx.doi.org/10.1016/j.cattod.2014.05.037
0920-5861/

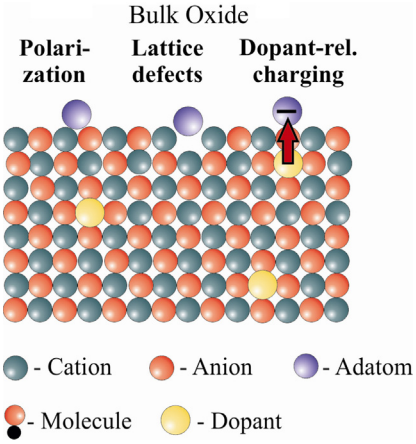

Fig. 1. Different binding mechanisms of adsorbates on bulk oxides.

ad-species has been revealed, the direction of which is given by the nature of the dopant in conjunction with the electronegativity of the adsorbate. Again, charge exchange is connected with a considerable increase of the adsorption strength [32]. In the following, we will substantiate those general considerations on the basis of two case studies carried out in the authors laboratory.

2. VO_x oxide clusters supported on CeO_2(1 1 1) for methanol oxidation [3]

In the spirit of what was argued in the introduction, we have studied the deposition of vanadium onto a thin CeO_2(1 1 1) film grown on Ru(0 0 0 1). The film has been chosen such (5–8 O–Ce–O tri-layers), that the metal substrate does not influence the chemistry on the films surface in any noticeable way.

Recently, comprehensive studies of the structure of vanadia clusters on CeO_2(1 1 1) thin films as a function of vanadia coverage have been performed [3].

Fig. 2 shows STM images of VO_x/CeO_2(1 1 1) surface at increasing vanadia coverage, that is, from 0.1 to 4.3 atom/nm^2. Random distribution of vanadia species together with the absence of preferential nucleation sites suggests a strong interaction between vanadia species and the underlying ceria support. In the atomically resolved image (Fig. 2a), the protruding spots (ca. 3 Å in diameter and 1.2 Å in height) appear to be monomers positioned atop protrusions in the ceria substrate. Increasing vanadia coverage first resulted in a higher density of monomeric species and the simultaneous formation of dimers, trimers, and ill-defined large aggregates with a relatively broad size distribution, which are indicative for kinetically limited growth of the vanadia particles deposited at room temperature. The monomeric species are thermally the least stable. Annealing to 700 K caused monomers to sinter, ultimately producing vanadia trimers and heptamers, particularly at higher coverage. The distance between the protrusions within the trimers and heptamers (~3.9 Å) is basically the same as measured on the pristine ceria films. The apparent height of these islands, ca. 1.3 Å, is about the same as for monomers. The respective IRA spectra revealed only bands at 1000–1040 cm^{-1}, which, combined with the XPS results showing vanadium only in a +5 oxidation state, strongly suggest these species to be vanadyls (V=O) in nature. The IRAS band shifts from 1006 cm^{-1} for monomers to 1033 cm^{-1} for trimers and further to 1040 cm^{-1} for heptamers and larger oligomers (see Fig. 2c), ultimately approaching the frequencies (~1045 cm^{-1}) observed for vanadia three-dimensional nanoparticles supported on alumina and silica thin films [19,22]. This shift is characteristic for the onset of dipole coupling between neighboring V=O groups in the oligomers and is fully supported by DFT calculations [48,56]. Therefore, the presnr model systems allowes one to establish a direct structure–spectroscopy correlation for oxide supported vanadia clusters.

These well-defined systems were further studied with respect to oxidative dehydrogenation of methanol with the aim to understand the support effects observed on this reaction on the real catalysts [12]. Methanol oxidation on vanadia supported on both CeO_2(1 1 1) single crystal and polycrystalline ceria has previously been studied by the group of Vohs [13,48,55,56].

We have reported TPD spectra of methanol on ceria supported vanadia have been reported as a function of vanadia coverage [2]. The pristine CeO_2(1 1 1) surface of a film grown on Ru(0 0 0 1) shows a formaldehyde desorption signal at ~565 K. In the presence of vanadia, the desorption peak shifts to ~590 K. Note that in those experiments methanol was exposed to the sample at 300 K. As the coverage of vanadia increases, the integral intensity of the peak decreases and finally becomes negligible for the highest VO_x coverage. Two peaks related to the interaction of methanol with the vanadia/ceria surfaces appear at lower temperatures, (~370 K) and (~475 K).

It is clear that the formation of formaldehyde at 370 K is only observed at low and intermediate vanadia coverages, where monomeric vanadia-species were identified by IRAS. An STM study [3] showed that these species exhibit low thermal stability and that they sinter on heating. The peak at 475 K may partially be due to polymeric vanadia species, formed during the temperature ramp. For the highest coverage of vanadia, where large polymeric species dominate the surface structure prior to the temperature ramp, the peak at 475 K is shifted to about 500 K, and the overall reactivity diminishes. Therefore, low temperature reactivity observed for vanadia/ceria relates both to high dispersion of vanadia and to the degree of reduction of the ceria support close to V=O species, as indicated by photoelectron spectroscopy (not shown here).

Among several possible schemes for methanol adsorption, the one shown in Fig. 3a agrees best with the key experimental findings observed, that is, depletion of the V=O band in IRAS, V reduction in XPS, and available, reduced Ce sites in close proximity to V=O serving as binding sites for methoxy.

It appears that the support effects reported in the literature for real vanadia catalysts [4,39,49] are related to the stabilization of small and isolated vanadia species by reducible oxide supports. Another important factor that controls the reactivity is that ceria stabilizes vanadium in the form of vanadyls. To illustrate this, Fig. 3b shows the IRA spectra for the vanadium deposited at 100 K and then stepwise annealed to 300, and 700 K in UHV. The formation of V=O is clearly observed upon annealing to 300 K, which can only be explained by vanadyl oxygen incorporated from ceria support.

Further, annealing causes sintering, which is accompanied by the band shift toward higher frequencies, which agrees well with the data shown in Fig. 2.

The results of DFT calculations nicely prove this scenario [3]. When a V atom is deposited on the perfect CeO_2(1 1 1) surface, four electrons are transferred from V 3d states into Ce 4f states, thus creating four Ce^{3+} ions and leaving vanadium in the +4 oxidation state (see Fig. 3). There is, however, an isomeric structure of the V/CeO_2(1 1 1) system with 1.48 eV less energy, in which oxygen atoms have rearranged such that a vanadyl bond is formed and a subsurface oxygen defect is created in the third oxygen layer of ceria. Further DFT calculation by the Sauer group [33] reveal migration barriers for monomer species as high as 1.95 eV, which indicates that such species are kinetically "locked in".

In order to characterize point defects (oxygen vacancies) on and below the surface of CeO_2(1 1 1), we have used titration with Au atoms, which also reveal charge states, characteristic for specific defects [36,37]. The density of defects in the film was controlled by the final annealing step in the preparation. While annealing

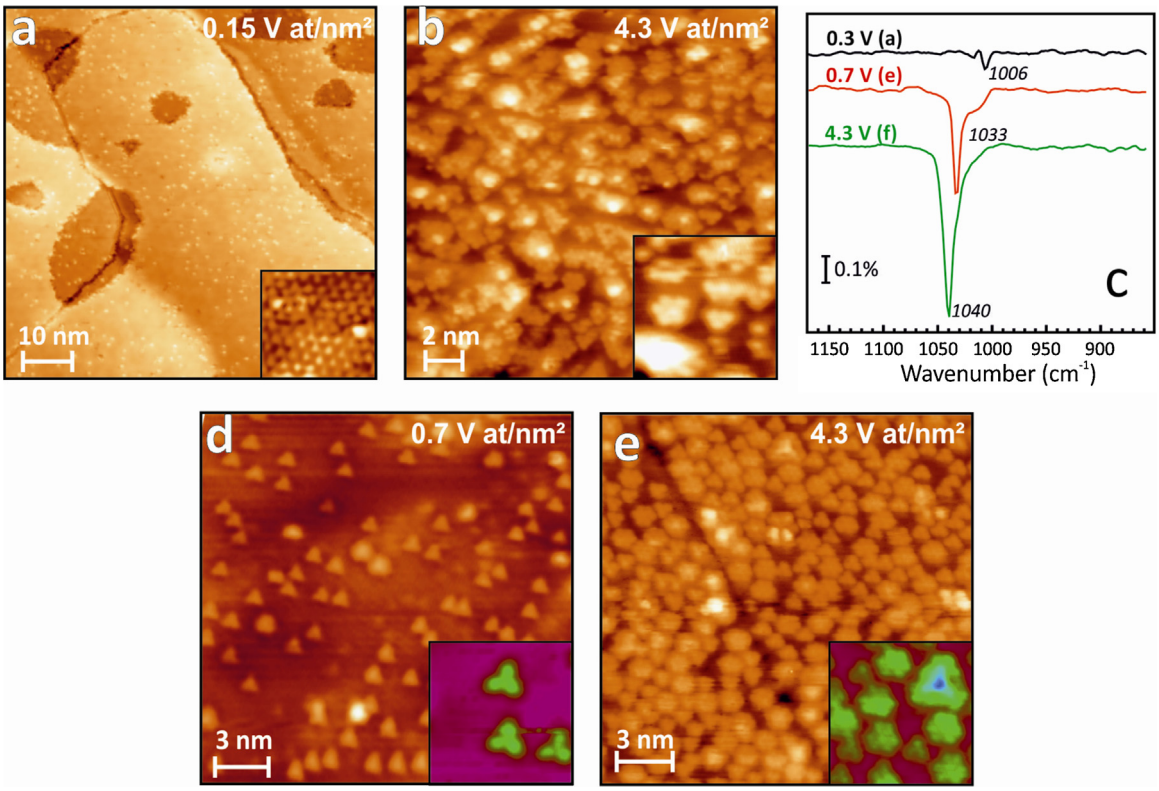

Fig. 2. (a and b) STM images of VO_x deposited on CeO_2(1 1 1) thin films in oxygen at 300 K with vanadia coverages of 0.15 at/nm^2 (a), and 4.3 at/nm^2 (b). STM images of samples (b) after annealing to 700 K are shown in (d) and (e), respectively. Insets show high-resolution images of the vanadia species such as monomers, dimers, trimers, and heptamers. IRA-spectra of the samples imaged in (a) and (d) and (e) are shown in (c) [2,3].

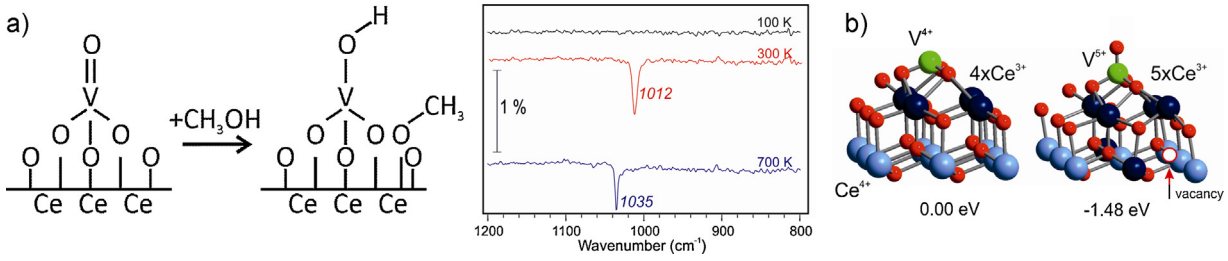

Fig. 3. (a) Scheme for methanol adsorption on V=O/CeO_2(1 1 1). (b) (*Left*) IRA spectra of VO_x/CeO_2(1 1 1) film as deposited at 100 K in UHV and annealed to the indicated temperature. (*Right*) The structures illustrating the formation of V=O with oxygen from the ceria support upon V atom deposition onto CeO_2(1 1 1) [16].

in oxygen triggered the formation of sub surface vacancies (V_{sub}), appearing as trifoliate depressions in empty-state (positive bias) images, vacuum annealing mainly produced surface defects (V_{surf}) [11,47]. The V_{surf} showed up as holes (not shown) and twofold or threefold maxima in filled and empty-state images, respectively (Fig. 4(b)).

The specific positive-bias contrast relates to the spill-out of 4f orbitals of adjacent Ce^{4+} ions, while Ce^{3+} species next to the vacancy appear slightly darker in the STM images [18]. The defect density was determined to be $\sim 5 \times 10^{12}$ cm^{-2} for V_{sub} at O_2-rich preparation conditions, and $\sim 5 \times 10^{13}$ cm^{-2} for V_{surf} defects formed upon 1000 K vacuum annealing. While the adsorption of Au atoms on defect free areas is mainly observed in O on-top positions, further binding geometries emerged in the presence of lattice defects. As expected, surface vacancies turned out to be effective traps for the Au atoms (Fig. 5) [34,59].

Such defect-bound species served as nucleation centers for incoming Au atoms and governed the aggregation processes on the surface [36]. However, also subsurface defects, more precisely the Ce^{3+} ions associated with them, were found to modify the adsorption behavior. Experimental evidence came from the unusual arrangement of Au atoms on oxide films with a high density of V_{sub} defects. At low exposure, up to 40% of the Au species appeared as characteristic pairs with a mean atom distance of 7.6 Å (two CeO_2 lattice parameters) (Fig. 5(a)). Note that even the shortest pair length of 4.8 Å observed here would be too large to be compatible with direct Au–Au coupling.

We therefore, based on DFT calculations carried out by the Sauer group, suggest that this unusual atom distribution is governed by defects in the ceria lattice. The atom pairs were found to be metastable, as they could be assembled to a single upright Au_2 dimer with a 3.0 V tip pulse [Fig. 5(d)]. Further manipulation experiments enabled us to determine the binding sites of the paired atoms by desorbing them via high bias scanning. In a few successful examples, we could identify a subsurface vacancy in close vicinity to the Au pair, suggesting an involvement of this defect type in the pair formation (Fig. 6(c)). This idea is supported by a statistical analysis of our data that revealed a direct dependence of the number of Au pairs on the V_{sub} concentration in the surface [1]. Finally, all atoms in paired configurations but also a couple of isolated monomers

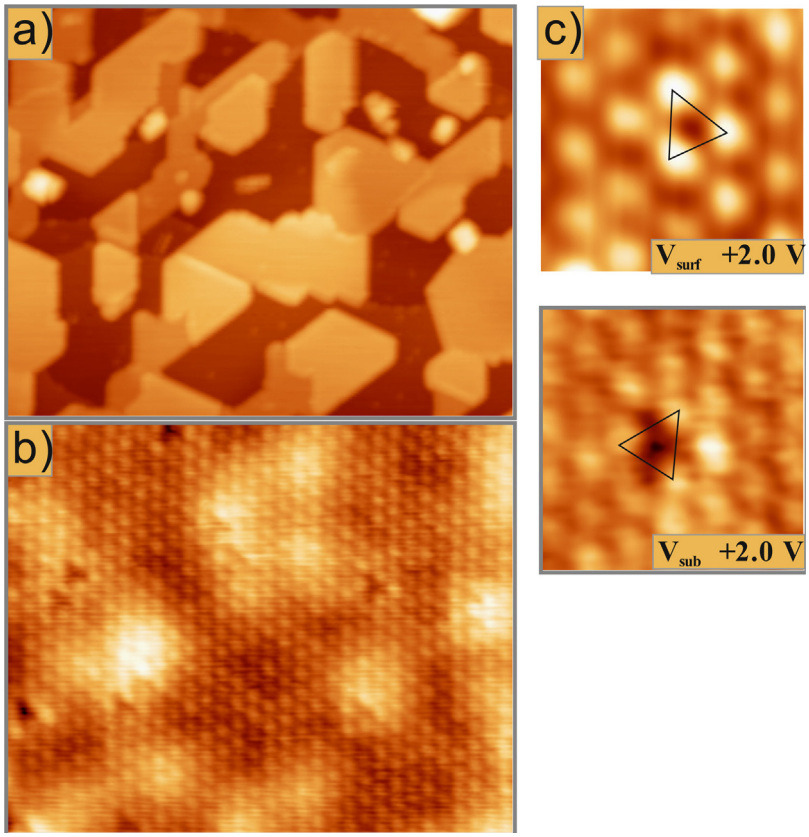

Fig. 4. (a) Atomically resolved STM image (10.5 nm × 8.5 nm) of a five trilayer thick CeO_2(1 1 1) film grown on Ru(0 0 0 1) (U_s = +2.0 V). (b) High-resolution images of surface (V_{surf}) and subsurface O vacancies (V_{sub}) measured at positive sample bias (2 nm × 2 nm). All STM data have been obtained at 25 pA current [37].

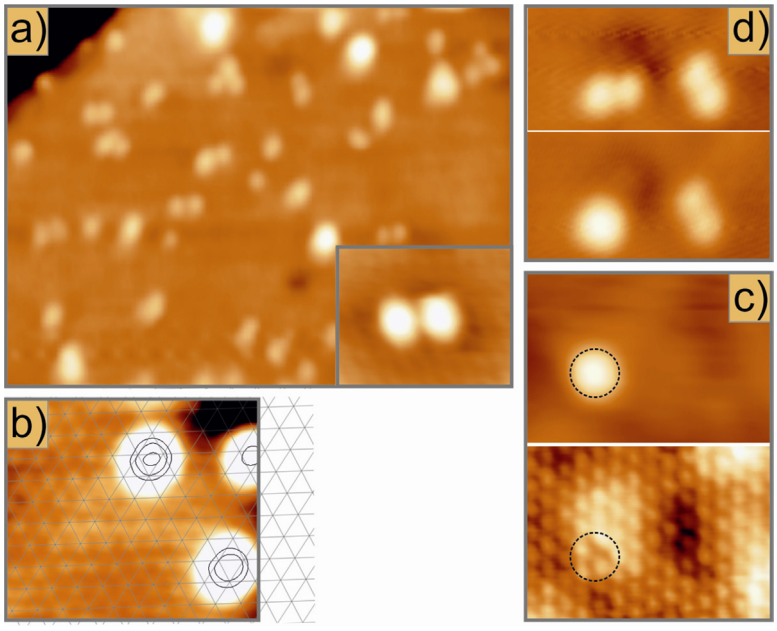

Fig. 5. (a) Ceria surface after dosing 0.05 mL of Au at 10 K (2.5 V, 26 nm × 20 nm). Note the abundance of atom pairs on the surface. The pair in the inset shows a pronounced sombrero shape, indicating its charged nature. (b) STM image showing the Ce sub-lattice and three Au atoms bound to regular O-top sites. (c) Au adatom bound to a subsurface defect, as deduced from the atomically resolved image taken after atom removal with the tip (both 4.2 nm × 3.0 nm). (d) Transformation of an Au atom pair into an upright standing dimer via a tip-voltage pulse (5.5 nm × 3.0 nm) [37].

featured a specific contrast in low bias images, characterized by a dark ring around the actual maximum (Fig. 5(a), inset). In earlier experiments on alumina [29] and magnesia films [46], such sombrero shapes were associated with charges on the adatoms, inducing a local bending of the surrounding oxide bands. We thus conclude that V_{sub} defects are not only responsible for the pair formation, but induce a charge transfer into the Au atoms as well. As a working hypothesis, we propose that the Au pairs result from

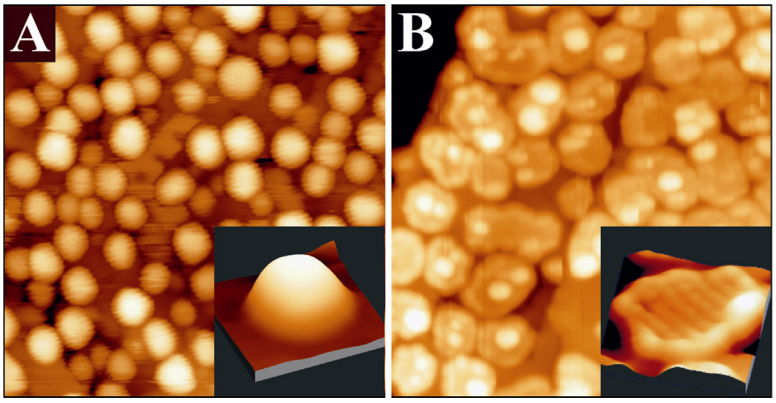

Fig. 6. STM images of 0.7 mL Au dosed onto (a) pristine and (b) doped CaO films (4.5 V, 50 nm × 50 nm). The insets display close-ups of two characteristic particles (−5.0 V, 10 nm × 10 nm) [42].

a titration of the Ce^{3+} surface species created by oxygen removal from the ceria lattice. It should be noted, that Au adsorption at higher coverage on defect free areas leads to very different adsorbate structures [36].

3. Oxygen adsorption on doped oxides

By studying charge transfer through ultrathin oxide films grown on metal supports we have demonstrated by a large number of studies in the past, the influence of the metal support on the morphology and particle growth mode on top of those films [21,29,31].

An interesting possibility to extend the concept of charge-mediated particle growth from thin, metal supported films to bulk oxides, where the metal support as a source of electrons is no longer available, is the insertion of suitable charge sources directly into the oxide material [7,8], preferentially into a near-surface region to allow for charge exchange with adsorbates. The fundamental approach to insert charge centers into a material is doping, and the underlying concepts have been introduced in the mature field of semiconductor technology [25]. Oxides, different from semiconductors, are subject to self-doping either by native defects or unwanted impurities, the concentration of which is difficult to control experimentally [51]. Both lattice defects and impurity ions may adopt different charge states in the oxide lattice [20,43], a variability that leads to pronounced compensation effects and is less common in semiconductors. Finally, dopants may be electrically inactive in a wide-gap insulator, as thermal excitation is insufficient to promote electrons from defect states into bulk bands. As a result, the excess charges remain trapped at the host ions and are unavailable for charge transfer. The following examples demonstrate, however, that doping may be used to control the growth of metals even on bulk- like oxide materials [17,23,26,30,35,38,50]. The underlying concepts are similar to those developed for thin films before [31].

In general, doping is carried out with impurity ions that adopt either a higher or lower valence state than the substituted ions in the host lattice. Whereas high-valence dopants may serve as charge donors and provide extra electrons, under-valent dopants exhibit acceptor character and may accommodate electrons from suitable adsorbates.

The impact of doping on the growth morphology of gold nanoparticles has first been realized for crystalline CaO(0 0 1) doped with Mo in the sub-percent range [42]. On the doped oxide, gold was found to spread out into flat monolayer islands, while the conventionally expected 3D growth prevailed on pristine, non-doped CaO material (Fig. 6).

Evidently, the Mo dopants are responsible for the 2D growth morphology, as the bare CaO(0 0 1) surface interacts with gold only weakly. Doped bulk oxides display, in many respects, similar adsorption properties as ultrathin oxide films, as anticipated above. In both systems, excess electrons are transferred into the ad-species. Whereas for ultrathin films, the extra electrons are provided by the metal substrate below, doped oxides contain intrinsic charge sources in the form of alio-valent impurity ions. Thin oxide films grown on metal single crystals are mainly of academic interest, as they provide easy access to the properties of oxide materials via conventional surface science techniques. Doped oxides, on the other hand, are of practical relevance for instance in heterogeneous catalysis. As shown in this section, over-valent dopants are able to change the particles equilibrium shape from 3D to 2D, which is expected to change the reactivity pattern of the metal-oxide system. Moreover, charge transfer from electron-rich dopants might be a suitable pathway to activate small molecules, such as oxygen or methane, as discussed next.

Using scanning tunneling microscopy and density functional theory, evidence is provided that strongly bound O_2^- species with high susceptibility for dissociation form even on chemically inert CaO(0 0 1) surfaces after the material has been doped with Mo ions. Fig. 7 displays STM images of such a doped CaO(0 0 1) film before and after exposure to O_2 for weakly and doped CaO films.

Fig. 7 displays weakly and strongly doped CaO films after exposure to 5 L O_2 at 20 K. Whereas Mo-poor films are unable to bind oxygen, a rather high adsorbate concentration is found for Mo-rich preparations, indicating the crucial role of the dopants for binding.

To correlate the Mo concentration with the CaO reactivity toward oxygen, the position of the oxide conduction band with respect to the Fermi level can be used as a descriptor. With increasing donor concentration, the band position experiences a downshift, as electrons are transferred from interfacial Mo species to the metal substrate below [41]. This charge flow generates a positive interface dipole between oxide film and metal support that shifts the vacuum level and the oxide conduction band to lower energy (Fig. 7b). A steep onset in the O_2 adsorption probability is now observed when the band edge drops below 3.0 eV, while films with a band position higher than 4.0 eV are unable to bind oxygen. Again, electron donation from the Mo impurities is the crucial requirement for molecular activation.

Although the band position is a nonlocal parameter, dopants and O_2 molecules are expected to interact directly with each other and not through a delocalized charge background. Experimental evidence comes from O desorption experiments, in which isolated molecules are removed from the surface by a bias pulse with the STM tip. In 50% of those experiments, a Mo donor is detected below

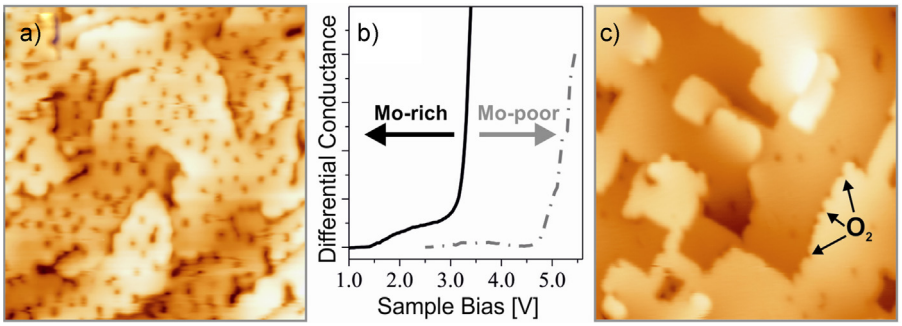

Fig. 7. (a and c) STM images of strongly and weakly doped CaO films after exposure to 5 L O_2 @ 20 K (40 nm × 40 nm). The O_2 adsorption probability correlates with the position of the CaO conduction band, as measured with dI/dV spectroscopy (b) Step edges are preferred O_2 binding sites only on weakly doped films (see arrows in c) [9].

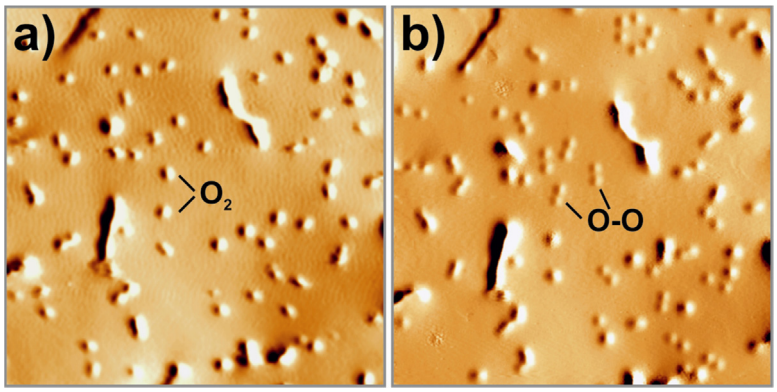

Fig. 8. STM images of the same O_2-covered region of Mo-doped CaO taken (a) before and (b) after multiple scans at 4.0 V (3.3 V, 40 nm × 40 nm). Note the dissociation of most molecules into atom pairs upon electron injection from the tip. While atoms appear with pronounced sombrero shapes at higher bias, the molecules are imaged as deep depressions in the surface [9].

the molecule by a characteristic feature in the STM image. Interestingly, the dopant never occupies a position directly in the top layer but sits in sub-surface oxide planes, as deduced from the diameter of characteristic charging rings emerging in the STM images [6]. It is concluded that the Mo ions are able to exchange charges with the surface O_2 molecules even over distances as large as 1 nm. A last experimental hint for O_2^- formation on doped CaO films comes from the facile dissociation of the molecules, which proceeds with close to 100% probability when 4.0 eV electrons are injected from the tip into the surface (1 min @ 20 pA) (Fig. 8).

The bond cleavage occurs as a second electron enters the antibonding states of the already weakened superoxo species. The electron transfer between Mo donors and O_2 acceptors has been corroborated with DFT calculations performed at the B3LYP + D level. On non-doped CaO(0 0 1), a neutral O_2 molecule binds with 13 kJ mol^{-1} (mostly from dispersion forces) to a Ca–Ca bridge position, while Ca^{2+} top sites are less preferred. In contrast, an O_2^- species binds to the same bridge site with a binding energy of 87 kJ mol^{-1}, when a Mo^{3+} ion is present in the third subsurface plane. The charge transfer to oxygen becomes even more favorable for Mo^{2+} donors in the oxide film, given their low ionization energy [42]. Further evidence for the formation of superoxo species comes from the bond elongation (121–133 pm) and the reduced stretching frequency (1537–1200 cm^{-1}) computed for O_2 molecules on the doped oxide. A lower apparent dissociation barrier was calculated by the Sauer group for superoxo species on doped CaO (66 kJ mol^{-1}) compared to that of neutral O_2 on pristine CaO (110 kJ mol^{-1}), following the trend observed experimentally. The O_2^- on Mo-doped CaO is bound with an energy of 90 kJ mol^{-1}, and is hence stable at room temperature. Moreover, the species is prone to dissociation into atomic oxygen on the doped surface. It is concluded that dopants may play a pivotal role in the activation of hydrocarbons on wide-band-gap oxides. The latter has been confirmed in an experimental study of the Schlögl group, which represents a synthetic masterpiece, and demonstrates an unusually high reaction yield for the oxidative coupling of methane over Fe-doped MgO powder [40].

4. Synopsis

We have demonstrated that model studies using systems with reduced complexity allow us to identify specific aspects in structure–spectroscopy and structure–reactivity relations, which would be very difficult, if not impossible, to isolate in a real catalytic material. By creating materials, which are suitable to be investigated via the tool box of surface science we showed unprecedented structural information for vanadia clusters on a ceria surface with well-defined defect structures, and the relation to its reactivity toward methanol oxidation. In a second case study we used the knowledge deduced from our studies on metal supported ultrathin films, and the electron transfer through the films, to propose that dopants in an oxide support might be the source of charge similar to the metal support underneath the ultrathin film. In a case study, Mo dopants in CaO are used to activate oxygen molecules on a defect free oxide surface. In a recent study the Schlögl group has presented [40] oxidative methane coupling studies on Fe doped MgO material which indicate the appropriateness of those model studies.

Acknowledgments

The authors are grateful to all members in the department of chemical physics of the Fritz Haber Institute for their contributions.

We thank the DFG for support through the cluster of excellence UniCat, administrated at the Technische Universität Berlin, as well as the Fonds der Chemischen Industrie.

In particular, we would like to acknowledge the contributions from our collaborating theory groups (Joachim Sauer, Gianfranco Pacchioni, Hannu Häkkinen) who provided impact without which it would been impossible to reach the conclusions.

References

[1] See Supplemental Material at http://link.aps.org/supplemental/10.1103/PhysRevLett.111.206101 for statistical analysis of defect versus Au-pair numbers, computational details, and atomic coordinates used in the calculations.
[2] H.L. Abbott, A. Uhl, M. Baron, Y. Lei, R.J. Meyer, D.J. Stacchiola, O. Bondarchuk, S. Shaikhutdinov, H.J. Freund, Relating methanol oxidation to the structure of ceria-supported vanadia monolayer catalysts, J. Catal. 272 (2010) 82–91.
[3] M. Baron, H. Abbott, O. Bondarchuk, D. Stacchiola, A. Uhl, S. Shaikhutdinov, H.-J. Freund, C. Popa, M.V. Ganduglia-Pirovano, J. Sauer, Resolving the atomic structure of vanadia monolayer catalysts: monomers, trimers, and oligomers on ceria, Angew. Chem. Int. Ed. 48 (2009) 8006–8009.
[4] L.J. Burcham, G. Deo, X.T. Gao, I.E. Wachs, In situ IR, Raman, and UV–vis DRS spectroscopy of supported vanadium oxide catalysts during methanol oxidation, Top. Catal. 11 (2000) 85–100.
[5] J.L. Callahan, R.K. Grasselli, A selectivity factor in vapor-phase hydrocarbon oxidation catalysis, AIChE J. 9 (1963) 755–760.
[6] Y. Cui, N. Nilius, H.-J. Freund, S. Prada, L. Giordano, G. Pacchioni, Controlling the charge state of singe mo-dopants in a CaO thin film, Phys. Rev. Lett. (2013) (submitted for publication).
[7] Y. Cui, N. Nilius, H.-J. Freund, S. Prada, L. Giordano, G. Pacchioni, Controlling the charge state of single Mo dopants in a CaO film, Phys. Rev. B 88 (2013) 205421.
[8] Y. Cui, N. Nilius, X. Shao, M. Baldofski, J. Sauer, H.-J. Freund, Adsorption, activation and dissociation of oxygen on doped oxides, Angew. Chem. Int. Ed. (2013) (submitted for publication).
[9] Y. Cui, X. Shao, M. Baldofski, J. Sauer, N. Nilius, H.-J. Freund, Adsorption, activation, and dissociation of oxygen on doped oxides, Angew. Chem. Int. Ed. 52 (2013) 11385–11387, http://dx.doi.org/10.1002/anie.201305119.
[10] G. Ertl, H. Knözinger, F. Schueth, J. Weitkamp, Handbook of Heterogeneous Catalysis, 2nd compl. rev. and enlarged edition, VCH, Weinheim, 2008.
[11] F. Esch, S. Fabris, L. Zhou, T. Montini, C. Africh, P. Fornasiero, G. Comelli, R. Rosei, Electron localization determines defect formation on ceria substrates, Science 309 (2005) 752–755.
[12] M. Ettler, H. Timmermann, J. Malzbender, A. Weber, N.H. Menzler, Durability of Ni anodes during reoxidation cycles, J. Power Sources 195 (2010) 5452–5467.
[13] T. Feng, J.M. Vohs, A TPD study of the partial oxidation of methanol to formaldehyde on CeO_2-supported vanadium oxide, J. Catal. 221 (2004) 619–629.
[14] H.-J. Freund, M. Heyde, N. Nilius, S. Schauermann, S. Shaikhutdinov, M. Sterrer, Model studies on heterogeneous catalysts at the atomic scale: from supported metal particles to two-dimensional zeolites, J. Catal. 308 (2013) 154–167.
[15] H.J. Freund, Model studies in heterogeneous catalysis, Chem. Eur. J. 16 (2010) 9384–9397.
[16] M.V. Ganduglia-Pirovano, C. Popa, J. Sauer, H. Abbott, A. Uhl, M. Baron, D. Stacchiola, O. Bondarchuk, S. Shaikhutdinov, H.-J. Freund, Role of ceria in oxidative dehydrogenation on supported vanadia catalysts, J. Am. Chem. Soc. 132 (2010) 2345–2349.
[17] T. Ito, J. Wang, C.H. Lin, J.H. Lunsford, Oxidative dimerization of methane over a lithium-promoted magnesium oxide catalyst, J. Am. Chem. Soc. 107 (1985) 5062–5068.
[18] J.-F. Jerratsch, X. Shao, N. Nilius, H.-J. Freund, C. Popa, M.V. Ganduglia-Pirovano, A.M. Burow, J. Sauer, Electron Localization in Defective Ceria Films: A Study with Scanning-Tunneling Microscopy and Density-Functional Theory, Phys. Rev. Lett. 106 (2011) 246801.
[19] S. Kaya, Y.N. Sun, J. Weissenrieder, D. Stacchiola, S. Shaikhutdinov, H.J. Freund, Ice-assisted preparation of silica-supported vanadium oxide particles, J. Phys. Chem. C 111 (2007) 5337–5344.
[20] H.Y. Kim, H.M. Lee, R.G.S. Pala, V. Shapovalov, H. Metiu, CO oxidation by rutile TiO_2(1 1 0) doped with V, W, Cr, Mo, and Mn, J. Phys. Chem. C 112 (2008) 12398–12408.
[21] M. Kulawik, N. Nilius, H.J. Freund, Influence of the metal substrate on the adsorption properties of thin oxide layers: Au atoms on a thin alumina film on NiAl(1 1 0), Phys. Rev. Lett. 96 (2006) 036103.
[22] N. Magg, B. Immaraporn, J.B. Giorgi, T. Schroeder, M. Bäumer, J. Dobler, Z.L. Wu, E. Kondratenko, M. Cherian, M. Baerns, P.C. Stair, J. Sauer, H.J. Freund, Vibrational spectra of alumina- and silica-supported vanadia revisited: an experimental and theoretical model catalyst study, J. Catal. 226 (2004) 88–100.
[23] N. Mammen, S. Narasimhan, S.D. Gironcoli, Tuning the morphology of gold clusters by substrate doping, J. Am. Chem. Soc. 133 (2011) 2801–2803.
[24] Y. Martynova, B.H. Liu, M.E. McBriarty, I.M.N. Groot, M.J. Bedzyk, S. Shaikhutdinov, H.J. Freund, CO oxidation over ZnO films on Pt(1 1 1) at near-atmospheric pressures, J. Catal. 301 (2013) 227–232.
[25] W. Mönch, Semiconductor Surfaces and Interfaces, Springer, Berlin/Heidelberg, 1995.
[26] A. Nambu, J. Graciani, J.A. Rodriguez, Q. Wu, E. Fujita, J.F. Sanz, N doping of TiO_2(1 1 0): photoemission and density-functional studies, J. Chem. Phys. 125 (2006) 094706.
[27] K.M. Neyman, N. Roesch, Co bonding and vibrational-modes on a perfect Mgo (0 0 1) surface – Lcgto-Ldf model cluster investigation, Chem. Phys. 168 (1992) 267–280.
[28] K.M. Neyman, S.P. Ruzankin, N. Rösch, Adsorption of CO molecules on a MgO(0 0 1) surface. Model cluster density functional study employing a gradient-corrected potential, Chem. Phys. Lett. 246 (1995) 546–554.
[29] N. Nilius, M.V. Ganduglia-Pirovano, V. Brázdová, M. Kulawik, J. Sauer, H.J. Freund, Counting electrons transferred through a thin alumina film into Au chains, Phys. Rev. Lett. 100 (2008), 096802-096801-096804.
[30] M. Nolan, V.S. Verdugo, H. Metiu, Vacancy formation and CO adsorption on gold-doped ceria surfaces, Surf. Sci. 602 (2008) 2734–2742.
[31] G. Pacchioni, H. Freund, Electron transfer at oxide surfaces. The MgO paradigm: from defects to ultrathin films, Chem. Rev. 113 (2012) 4035–4072.
[32] G. Pacchioni, L. Giordano, M. Baistrocchi, Charging of metal atoms on ultrathin MgO/Mo(1 0 0) films, Phys. Rev. Lett. 94 (2005) 226104.
[33] J. Paier, T. Kropp, C. Penschke, J. Sauer, Stability and migration barriers of small vanadium oxide clusters on the CeO_2(1 1 1) surface studied by density functional theory, Faraday Discuss. 162 (2013) 233–245.
[34] J. Paier, C. Penschke, J. Sauer, Oxygen defects and surface chemistry of ceria: quantum chemical studies compared to experiment, Chem. Rev. 113 (2013) 3949–3985.
[35] R.G.S. Pala, H. Metiu, The structure and energy of oxygen vacancy formation in clean and doped, very thin films of ZnO, J. Phys. Chem. C 111 (2007) 12715–12722.
[36] Y. Pan, Y. Cui, C. Stiehler, N. Nilius, H.-J. Freund, Gold adsorption on CeO_2 thin films grown on Ru(0 0 0 1), J. Phys. Chem. C 117 (2013) 21879–21885.
[37] Y. Pan, N. Nilius, H.-J. Freund, J. Paier, C. Penschke, J. Sauer, Titration of Ce^{3+} ions in the CeO_2(1 1 1) surface by Au adatoms, Phys. Rev. Lett. 111 (2013) 206101.
[38] J.A. Rodriguez, J.C. Hanson, J.-Y. Kim, G. Liu, A. Iglesias-Juez, M. Fernández-García, Properties of CeO_2 and $Ce_{1-x}Zr_xO_2$ nanoparticles: X-ray absorption near-edge spectroscopy, density functional, and time-resolved X-ray diffraction studies, J. Phys. Chem. B 107 (2003) 3535–3543.
[39] Y. Romanyshyn, S. Guimond, H. Kuhlenbeck, S. Kaya, R.P. Blum, H. Niehus, S. Shaikhutdinov, M. Simic-Milosevic, N. Nilius, H.J. Freund, M.V. Ganduglia-Pirovano, R. Fortrie, J. Döbler, J. Sauer, Selectivity in methanol oxidation as studied on model systems involving vanadium oxides, Top. Catal. 50 (2008) 106–115.
[40] P. Schwach, M.G. Willinger, A. Trunschke, R. Schlögl, Methane coupling over magnesium oxide: how doping can work, Angew. Chem. Int. Ed. 52 (2013) 11381–11384.
[41] X. Shao, N. Nilius, H.-J. Freund, Li/Mo codoping of CaO films: a means to Tailor the equilibrium shape of Au deposits, J. Am. Chem. Soc. 134 (2012) 2532–2534.
[42] X. Shao, S. Prada, L. Giordano, G. Pacchioni, N. Nilius, H.-J. Freund, Tailoring the shape of metal ad-particles by doping the oxide support, Angew. Chem. Int. Ed. 50 (2011) 11525–11527.
[43] V. Shapovalov, H. Metiu, Catalysis by doped oxides: CO oxidation by $Au_xCe_{1-x}O_2$, J. Catal. 245 (2007) 205–214.
[44] M. Sterrer, H.-J. Freund, Towards realistic surface science models of heterogeneous catalysts: influence of support hydroxylation and catalyst preparation method, Catal. Lett. 143 (2013) 375–385.
[45] M. Sterrer, T. Risse, M. Heyde, H.-P. Rust, H.-J. Freund, Crossover from three-dimensional to two-dimensional geometries of Au nanostructures on thin MgO(0 0 1) films: a confirmation of theoretical predictions, Phys. Rev. Lett. 98 (2007) 206103.
[46] M. Sterrer, T. Risse, U. Martinez Pozzoni, L. Giordano, M. Heyde, H.-P. Rust, G. Pacchioni, H.-J. Freund, Control of the charge state of metal atoms on thin MgO films, Phys. Rev. Lett. 98 (2007) 096107.
[47] S. Torbrügge, M. Reichling, A. Ishiyama, S. Morita, Ó. Custance, Evidence of subsurface oxygen vacancy ordering on reduced CeO_{2}(1 1 1), Phys. Rev. Lett. 99 (2007) 056101.
[48] J.M. Vohs, T. Feng, G.S. Wong, Comparison of the reactivity of high-surface area, monolayer vanadia/ceria catalysts with vanadia/CeO_2(1 1 1) model systems, Catal. Today 85 (2003) 303–309.
[49] I.E. Wachs, Recent conceptual advances in the catalysis science of mixed metal oxide catalytic materials, Catal. Today 100 (2005) 79–94.
[50] J.X. Wang, J.H. Lunsford, Characterization of [Li+O] centers in lithium-doped magnesium oxide catalysts, J. Phys. Chem. 90 (1986) 5883–5887.
[51] S. Wendt, P.T. Sprunger, E. Lira, G.K.H. Madsen, Z. Li, J.Ø. Hansen, J. Matthiesen, A. Blekinge-Rasmussen, E. Lægsgaard, B. Hammer, F. Besenbacher, The role of interstitial sites in the Ti3d defect state in the band gap of titania, Science 320 (2008) 1755–1759.
[52] R. Wichtendahl, M. Rodriguez-Rodrigo, U. Härtel, H. Kuhlenbeck, H.-J. Freund, TDS study of the bonding of CO and NO to vacuum-cleaved NiO(1 0 0), Surf. Sci. 423 (1999) 90–98.
[53] R. Wichtendahl, M. Rodriguez-Rodrigo, U. Härtel, H. Kuhlenbeck, H.J. Freund, Thermodesorption of CO and NO from vacuum-cleaved NiO(1 0 0) and MgO(1 0 0), Phys. Status Solidi A 173 (1999) 93–100.
[54] F. Winkelmann, S. Wohlrab, J. Libuda, M. Bäumer, D. Cappus, M. Menges, K. Al-Shamery, H. Kuhlenbeck, H.J. Freund, Adsorption on oxide surfaces: structure and dynamics, Surf. Sci. 307–309 (1994) 1148.
[55] G.S. Wong, M.R. Concepcion, J.M. Vohs, Oxidation of methanol to formaldehyde on vanadia films supported on CeO_2(1 1 1), J. Phys. Chem. B 106 (2002) 6451–6455.

[56] G.S. Wong, D.D. Kragten, J.M. Vohs, The oxidation of methanol to formaldehyde on TiO_2(1 1 0)-supported vanadia films, J. Phys. Chem. B 105 (2001) 1366–1373.
[57] Y. Xu, J. Li, Y. Zhang, W. Chen, CO adsorption on MgO(0 0 1) surface with oxygen vacancy and its low-coordinated surface sites: embedded cluster model density functional study employing charge self-consistent technique, Surf. Sci. 525 (2003) 13–23.
[58] M. Yulikov, M. Sterrer, M. Heyde, H.P. Rust, T. Risse, H.-J. Freund, G. Pacchioni, A. Scagnelli, Binding of single gold atoms on thin MgO(0 0 1) films, Phys. Rev. Lett. 96 (2006) 146804.
[59] C. Zhang, A. Michaelides, S.J. Jenkins, Theory of gold on ceria, Phys. Chem. Chem. Phys. 13 (2011) 22–33.